Cardiac specific expression of ΔH2-R15 mini-dystrophin normalized all ECG abnormalities and the end-diastolic volume in a 23-m-old mouse model of Duchenne dilated cardiomyopathy

Nalinda B. Wasala[1], Jin-Hong Shin[1, 2], Yi Lai[1], Yongping Yue[1], Federica Montanaro[3], Dongsheng Duan[1, 4, 5, 6 *]

1. Department of Molecular Microbiology and Immunology, School of Medicine, The University of Missouri, Columbia, MO 65212, USA
2. Current address: Pusan National University Yangsan Hospital, Yangsan, Republic of Korea
3. Dubowitz Neuromuscular Centre, Molecular Neurosciences Section, Developmental Neurosciences Programme, UCL Great Ormond Street Institute of Child Health, London, WC1N 1EH, UK
4. Department of Neurology, School of Medicine, The University of Missouri, Columbia, MO 65212, USA
5. Department of Bioengineering, The University of Missouri, Columbia, MO 65212, USA
6. Department of Biomedical Sciences, College of Veterinary Medicine, The University of Missouri, Columbia, MO 65212, USA

*Corresponding Address: Dongsheng Duan PhD
Dep. of Molecular Microbiology and Immunology
One Hospital Dr.
Columbia, MO 65212
Phone: 573-884-9584
Fax: 573-882-4287
Email: duand@missouri.edu

Short title: Inclusion of R16-19 enhanced heart rescue

Abstract

Heart disease is a major health threat for Duchenne/Becker muscular dystrophy patients and carriers. Expression of a 6 to 8-kb mini-dystrophin gene in the heart holds promise to dramatically change the disease course. However the mini-dystrophin gene cannot be easily studied with adeno-associated virus (AAV) gene delivery because the size of the minigene exceeds AAV packaging capacity. We previously studied cardiac protection of the ΔH2-R19 minigene using the cardiac specific transgenic approach. Although this minigene fully normalized skeletal muscle force, it only partially corrected ECG and heart hemodynamics in dystrophin-null mdx mice that had moderate cardiomyopathy. Here, we evaluated the ΔH2-R15 minigene using the same transgenic approach in mdx mice that had more severe cardiomyopathy. In contrast to the ΔH2-R19 minigene, the ΔH2-R15 minigene carries dystrophin spectrin-like repeats 16 to 19 (R16-19), a region that has been suggested to protect the heart in clinical studies. Cardiac expression of the ΔH2-R15 minigene normalized all aberrant ECG changes and improved hemodynamics. Importantly, it corrected the end-diastolic volume, an important diastolic parameter not rescued by ΔH2-R19 mini-dystrophin. We conclude that that ΔH2-R15 mini-dystrophin is a superior candidate gene for heart protection. This finding has important implications in the design of the mini/micro-dystrophin gene for Duchenne cardiomyopathy therapy.

Mary Ann Liebert, Inc., 140 Huguenot Street, New Rochelle, NY 10801

Introduction

Loss of dystrophin results in Duchenne muscular dystrophy (DMD). While skeletal muscle presentations start at the toddler age, symptoms of myocardial involvement are rarely seen before teenage. Despite the later onset, up to 40% of patients may die from heart failure and/or sudden cardiac death [1-3]. Currently, there is no etiology-based treatment for Duchenne cardiomyopathy. Gene therapy may solve the fundamental problem of dystrophin deficiency [4-6]. Some serotypes of adeno-associated virus (AAV) have the intrinsic property of reaching all body muscles (including the heart) after a single intravascular delivery [7-11]. This makes AAV a favored vector for DMD gene therapy. Unfortunately, the dystrophin gene is one of the largest genes in the genome and AAV is one of the smallest viruses. As a matter of fact, the size of the full-length dystrophin coding sequence is about three times the size of the AAV genome. Development of minimized dystrophin may open the door for AAV-mediated DMD gene therapy.

Dystrophin is a 427-kD rod-shaped protein encoded by 79 exons. It has four major domains. The N-terminal domain interacts with filamentous cytoskeletal γ-actin. Immediately following the N-terminal domain is the rod domain which accounts for more than 70% of the molecular weight of dystrophin. The rod domain can be further divided in 24 spectrin-like repeats (R) and four intervening hinges (H). The rod domain contains the second actin-binding domain and neuronal nitric oxide synthase (nNOS) binding domain. Towards the carboxyl end is the cysteine-rich (CR) domain and the C-terminal domain. The CR domain interacts with transmembrane protein dystroglycan. The C-terminal domain binds to syntrophin and dystrobrevin. Abbreviated dystrophins have been generated largely based on our understanding of the structure-function relationship of dystrophin in skeletal muscle. Of particular interest is

the notion that most part of the rod domain can be deleted without significant consequences on function [12, 13]. A 6.2-kb Δ17-48 minigene was found in a 61-year-old ambulant patient [13]. The Chamberlain lab optimized this 6.2-kb minigene into the 6-kb ΔH2-R19 minigene. Transgenic expression of the ΔH2-R19 minigene yielded better skeletal muscle protection than the Δ17-48 minigene in dystrophin-null mdx mice. Importantly, ΔH2-R19 mini-dystrophin fully restored muscle force [12, 14]. In light of these encouraging skeletal muscle data on the ΔH2-R19 minigene [12, 14], we generated cardiac specific ΔH2-R19 min-dystrophin transgenic mdx mice [15]. We studied heart protection of ΔH2-R19 min-dystrophin in 21-m-old male mdx mice which show moderate cardiomyopathy [15-18]. In contrast to what was seen in skeletal muscle [12, 14], expression of ΔH2-R19 min-dystrophin in the heart only partially corrected ECG and cardiac hemodynamic deficiencies [15]. This unexpected result suggests that ΔH2-R19 mini-dystrophin may lack domain(s) important for heart function.

On reviewing the clinical literature, we found that patients with deletion mutations in the region of R16 to R19 often display early onset and/or more severe heart disease [19-33]. We wondered whether inclusion of R16-19 might lead to a better cardiac protection. To this end, we inserted R16-19 to ΔH2-R19 mini-dystrophin and made ΔH2-R15 mini-dystrophin (**Figure 1A**). We then generated cardiac-specific ΔH2-R15 mini-dystrophin transgenic mice [15]. To increase the stringency of the study, we focused on a more severe model that showed classic end-stage dilated cardiomyopathy found in human patients [16-18, 34]. Despite the fact that the ΔH2-R15 minigene was tested in mice with more severe heart disease, surprisingly, several physiological parameters that were not corrected by the ΔH2-R19 minigene in the less severe model were now normalized by ΔH2-R15 mini-dystrophin. Our results suggest that inclusion of R16-19 in synthetic mini-dystrophins can enhance cardiac rescue.

Materials and Methods

Experimental Animals. All animal experiments were approved by the institutional animal care and use committee and were in accordance with NIH guidelines. FVB mice were used as the wild type control mice. They were generated in a barrier facility using breeders purchased from The Jackson Laboratory (Bar Harbor, ME). Congenic FVB background mdx mice were generated as we described before [35]. The transgenic founder lines were generated on the FVB background at the University of Missouri transgenic core. These mice express the ΔH2-R15 mini-dystrophin gene under the transcriptional control of the cardiac muscle specific α-myosin heavy chain (αMHC) promoter. Mini-dystrophin transgenic mdx mice were generated by crossing transgenic found mice with FVB background mdx mice. Two founder lines (line 271 and line 272) were generated. In our studies, we combined the data from both lines in our result section because (1) we have previously shown that 5-fold to 50-fold transgenic over-expression of mini-dystrophin in the heart yielded similar protection and (2) we did not detect a statistically significant difference between these two lines **(Supplementary Table 1)**. Below we further clarify the source of the mice used in each figure. The representative images for transgenic mice in Figure 1 are from line 271 animals. For the ECG analysis (Figure 2) we have used mice n=22 from line 271 and n=10 from line 272. For the left ventricle hemodynamics (Figure 3) we have used n=19 from line 271 and n=6 from line 272. We have used n=3 from lines 271 and 272 for the western blot quantification shown in Figure 4. For the Supplementary figure 1, we have used n=2 from line 271 and n=1 from line 272. The average age of the mice was 23.3±0.20 and 22.9±.0.05 months for lines 271 and 272 respectively. For the Supplementary table 1, we have used n=19 from line 271 and n=6 from line 272. All mice were maintained in a specific-pathogen free animal care facility on a 12-hour light (25 lux):12-hour dark cycle with access to

food and water *ad libitum*. Mice were euthanized following functional assays to harvest tissues. All histology and physiology studies were performed in mice that were 23-m-old (23.22 ± 0.16 months) **(Table 1)**.

Morphological studies. Dystrophin expression was evaluated by immunofluorescence staining using three independent dystrophin monoclonal antibodies including Dys2 (1:30; Vector Laboratories), DysB (1:80, clone 34C5, IgG1; Novocastra) and Mandys8 (1:200; Sigma Aldrich). Dys2 and DysB react with ΔH2-R15 mini-dystrophin. Mandys8 recognizes an epitope in dystrophin repeat 11, which is absent in ΔH2-R15 mini-dystrophin [36, 37]. General histology was examined by hematoxylin and eosin (HE) staining. Fibrosis was examined by Masson trichrome staining as we described before [38]. Slides were viewed at the identical exposure setting using a Nikon E800 fluorescence microscope. Photomicrographs were taken with a QImage Retiga 1300 camera [38]. The fibrotic tissue deposition was quantified using photomicrographs of Masson trichrome stained images using Photoshop Software. Briefly, the measurement scale was set up for the relevant magnification for the microscope and using the lasso tool in Photoshop, the fibrotic area was marked in individual images. The fibrotic area from multiple images were averaged per individual animal and the total area of fibrosis is calculated for 3-4 animal for each strain.

Western blot. Whole heart and muscle lysate was prepared as we described before [39]. Briefly, the tissues were snap frozen in liquid nitrogen. The frozen tissue samples were ground to fine powder in liquid nitrogen followed by homogenization in a buffer containing 10% sodium dodecyl sulfate, 5mM ethylenediaminetetraacetic acid, 62.5mM Tris-HCl at pH6.8 and the

protease inhibitor cocktail (Roche, Indianapolis, IN). The crude lysates were heated at 95°C for 3 min, chilled on ice for 2 min and then centrifuged at 14,000 rpm for 2 min. Supernatant was collected as the whole muscle lysate. Protein concentration was measured using the DC protein assay kit (Bio-Rad, Hercules, CA). Dystrophin was detected with the Dys2 antibody (1:100, Novocastra). The calcium handling proteins were detected using antibodies against sarcoplasmic/endoplasmic reticulum calcium ATPase 2a (SERCA2a, 1:2,500 Badrilla, Leeds UK) and phospholamban (1:2,500 Badrilla, Leeds UK). Proteins involved in cellular signaling were detected using antibodies for c-jun N-terminal kinase (JNK1, 1:1,000 BD Pharmingen San Jose, CA), p38α (1:500, Santa Cruz Biotechnology, Dallas, TX), Akt (1:1,000, Cell Signaling Technology, Danvers, MA), and endothelin-A receptor (ET-A, 1:5,000, Abcam, Cambridge, MA). For the loading control, we used antibodies against glyceraldehyde 3-phosphate dehydrogenase (GAPDH, 1:3,000; Millipore, Billerica, MA) and vinculin (1:2,000, Abcam, Cambridge, MA).

Western blot quantification was performed using the LI-COR Image Studio Version 5.0.21 software (https://www.licor.com). The intensity of the respective protein band was normalized to the corresponding loading control in the same blot. The relative band intensity was normalized to the wild type control group.

ECG and hemodynamic assay. Cardiac functions were evaluated using our published protocols as described in the standard operating protocol in the *Cardiac Protocols for Duchenne Animal Models* (http://www.parentprojectmd.org/site/PageServer?pagename=Advance_researchers_sops)[40, 41]. Specifically, a 12-lead ECG assay was performed using a commercial system from AD

Instruments (Colorado Springs, CO) [38, 42]. The Q wave amplitude was determined using the lead I tracing. Other ECG parameters were analyzed using the lead II tracing. The QTc interval was determined by correcting the QT interval with the heart rate as described by Mitchell et al [43]. The cardiomyopathy index was calculated by dividing the QT interval by the PQ segment [44]. Left ventricular hemodynamics was evaluated using a closed chest approach as we have previously described [38, 40]. The resulting PV loops were analyzed with the PVAN software (Millar Instruments, Houston, TX).

Statistical analysis. Data from individual experimental subject are presented using the scatter plots. Data from the experimental group are presented as mean ± stand error of mean. One-way ANOVA with Bonferroni's multiple comparison analysis was performed using GraphPad PRISM software version 7.0 for Mac OSX (GraphPad Software, La Jolla California USA, www.graphpad.com). A $p < 0.05$ was considered statistically significant.

Results

Generation of αMHC.ΔH2-R15 mini-dystrophin transgenic mdx mice. To study the cardiac benefit of ΔH2-R15 mini-dystrophin, we generated cardiac specific αMHC.ΔH2-R15 minigene transgenic mice (**Figure 1A**). Cardiac specific expression was regulated by the αMHC promoter and the bovine growth hormone gene polyadenylation sequence. Two founder lines (line 271 and line 272) were generated on the FVB background and subsequently crossed to the FVB background mdx mice.

The progression of Duchenne cardiomyopathy undergoes several distinctive phases from pre-symptomatic stage to compensatory hypertrophic cardiomyopathy and eventually dilated cardiomyopathy [16, 17]. We recently discovered that only ≥21-m-old female mdx mice display severe end-stage dilated cardiomyopathy [18]. Hence, we focused the current study on 23-m-old female mdx mice. Cardiac expression of the ΔH2-R15 minigene was confirmed by dystrophin immunofluorescence staining in both founder lines using Dys2, DysB and Mandys8 antibodies. DysB and Dys2 recognize H1-R2 and the C-terminal domain, respectively while Mandys8 reacts with R11 which is absent in ΔH2-R15 mini-dystrophin **(Figure 1B)**. Heart lysate western blot revealed the right size band at levels 7.5 and 13-folds higher than that of full-length dystrophin in a normal heart **(Figure 1C)**. We have previously shown that transgenic mini-dystrophin expression in the mdx heart at 5- to 50-fold higher than that of full-length dystrophin in wild type mice yielded similar levels of histological and physiological rescue [45]. Hence, quantification data presented in the rest of the manuscript are from both lines. On HE staining and Masson trichrome staining, we detected nominal inflammation and fibrosis in the heart of αMHC.ΔH2-R15 mice **(Figure 1D, Supplementary Figure 1)**. On quantification, the fibrotic area in the heart of αMHC.ΔH2-R15 mice was significantly lower than that of mdx mice and actually it was

comparable to that of wild type mice **(Supplementary Figure 1)**. As expected, skeletal muscle of αMHC.ΔH2-R15 mice had no dystrophin expression and displayed characteristic degeneration and fibrosis comparable to those of mdx mice **(Figure 1E)** [35].

ΔH2-R15 mini-dystrophin normalized aberrant ECG changes. To determine therapeutic benefits on cardiac electrophysiology, we performed the 12-lead ECG assay [40, 41]. Except for the lack of tachycardia, we observed all other characteristic ECG abnormalities in transgene-negative mdx mice **(Figure 2)**. Specifically, the PR interval was significantly reduced, QRS duration and Mitchell's corrected QT (QTc) interval were significantly prolonged, the absolute value of the Q wave amplitude and the cardiomyopathy index were significantly increased **(Figure 2)**. These abnormal changes were completely corrected in αMHC.ΔH2-R15 mice **(Figure 2)**.

ΔH2-R15 mini-dystrophin prevented heart dilation. Hemodynamics was examined using left ventricular catheterization **(Figure 3, Supplementary Table 1)** [15, 42]. Similar to our previous report [18], we observed characteristic signs of dilated cardiomyopathy such as a significant increase of the end systolic volume and end diastolic volume in transgene-negative mdx mice **(Figure 3)**. Transgenic expression of ΔH2-R15 mini-dystrophin in the heart normalized the end-systolic volume, dP/dt maximum, end-diastolic volume and ejection fraction. A trend of improvement was also seen in the maximal pressure, dP/dt minimum, stroke volume and cardiac output **(Figure 3)**. Nevertheless, the isovolumetric relaxation time constant tau was not corrected **(Figure 3)**. In contrast, the mean tau value was significantly increased compared to that of wild type controls.

Anatomic examination revealed cardiac hypertrophy in αMHC.ΔH2-R15 mice. At the end of in-life study, we measured body weight (BW), heart weight (HW), ventricular weight (VW), tibia length (TL) and TA muscle weight (TW) **(Table 1)**. Compared to that of wild type control, TW was significantly reduced in αMHC.ΔH2-R15 mice, consistent with skeletal muscle disease-related limb muscle atrophy. Interestingly, HW and VW of αMHC.ΔH2-R15 mice were significantly (~14%) higher than those of wild type controls. The HW/TW and VW/TW ratios of αMHC.ΔH2-R15 mice were also significantly increased compared to those of wild type control mice, suggesting cardiac hypertrophy in αMHC.ΔH2-R15 mice. Since TW was affected by skeletal muscle disease, we evaluated TL normalized HW and VW [34, 46]. Compared to those of wild type control mice, the HW/TL and VW/TL ratios of αMHC.ΔH2-R15 mice were significantly higher, thus confirming cardiac hypertrophy in αMHC.ΔH2-R15 mice.

Evaluation of calcium handling proteins and cardiac hypertrophy related signaling proteins. To begin to understand the mechanisms of heart protection by ΔH2-R15 mini-dystrophin, we quantified the expression of SERCA2a and phospholamban, two important calcium handling proteins that are known to regulate heart contractility **(Figure 4)**. Compared to wild type control mice, both SERCA2a and phospholamban appeared reduced in mdx mice. Their levels were increased in αMHC.ΔH2-R15 mice but did not reach statistical significance.

Many signaling pathways have been implicated in cardiac hypertrophy (Reviewed in [47-51]). As the first step towards elucidation of the molecular processes underlying myocardial hypertrophy seen in αMHC.ΔH2-R15 mice, we examined several proteins in the mitogen-activated protein kinase (MAPK) pathway, Akt signaling and G-protein coupled receptor

signaling **(Figure 4)** [51-60]. These pathways have been implicated in either pathological or physiological cardiac hypertrophy. JNK1 and p38α are two important branches of the MAPK signaling cascade. We did not detect statistically significant difference **(Figure 4)**. Endothelin receptor A (ET-A) is a G-protein coupled receptor. Western blot on ET-A and Akt did not show noticeable trends **(Figure 4)**. In light of the substantial individual differences (especially for Akt) and the small sample size (n=3 for αMHC.ΔH2-R15 mice), we could not draw a solid conclusion on the involvement of the Akt signaling and G-protein receptor signaling.

Discussion

Two distinctive strategies have been used to study the structure-function relationship of dystrophin, namely the transgenic approach and AAV-mediated gene transfer. Systemic AAV delivery results in simultaneous transduction of both skeletal muscle and heart. This creates a challenge for sorting out cardiac specific effect because it is controversial whether treating skeletal muscle can reduce or aggravate heart disease in mdx mice [38, 61, 62]. To get a definitive answer on the cardiac specific effect, here we opted using the transgenic approach instead of AAV delivery to avoid confounding influences from skeletal muscle dystrophin expression.

Dystrophin is essential for the survival and function of both skeletal muscle and cardiac muscle. However, recent studies suggest that there may exist important differences between skeletal muscle dystrophin and cardiac dystrophin. For example, dystrophin directly binds to neuronal nitric oxide synthase (nNOS) in skeletal muscle and this interaction is critical to the sarcolemmal localization of nNOS in skeletal muscle [14, 63]. But in cardiac muscle, dystrophin dose not interact with nNOS and nNOS is localized in the sarcoplasmic reticulum and mitochondria in the heart [64-67]. Cytosolic nNOS compromises muscle function in mdx mice by inducing nitrosative stress but cytosolic over-expression of nNOS in the heart improves cardiac function in aged mdx mice [39, 67]. Cardiac dystrophin directly associates with myofibrils at the Z-disk but skeletal muscle dystrophin does not interact with myofibrils [68]. Recent proteomic studies have further identified cellular proteins that selectively interact with dystrophin in the heart but not in skeletal muscle [66]. Collectively, these observations suggest that dystrophin may play overlapping but distinctive roles in the heart and skeletal muscle. It is thus important to determine whether a therapeutic candidate dystrophin gene that can protect skeletal muscle can also protect the heart.

The ΔH2-R19 minigene and ΔH2-R15 minigene have both been shown to fully rescue skeletal muscle contractility [12, 14, 69]. Interestingly, cardiac-specific expression of the ΔH2-R19 minigene in transgenic mice failed to completely correct ECG abnormalities. In the hemodynamic assay, the ΔH2-R19 minigene also did not correct the end-diastolic volume, an important parameter in the context of Duchenne cardiomyopathy. It was unclear whether the ΔH2-R15 minigene can lead to better rescue. To address this question, we generated αMHC.ΔH2-R15 minigene transgenic mice **(Figure 1)** and then compared cardiac histopathology, anatomy and function among normal, transgene-positive and transgene negative mdx mice when they reached 23 months of age. In the absence of the minigene, mdx mice showed ECG and hemodynamic features that are characteristic for dilated cardiomyopathy **(Figures 2** and **3)**. All aberrant ECG changes were normalized in αMHC.ΔH2-R15 minigene transgenic mice **(Figure 2)**. On the cardiac catheter assay, the enlarged end-diastolic and end-systolic volumes were normalized by ΔH2-R15 mini-dystrophin, the reduced dP/dt max was returned to the wild type level, and ejection fraction was normalized **(Figure 3)**. Collectively, these results suggest that the ΔH2-R15 minigene is an outstanding candidate gene for treating Duchenne dilated cardiomyopathy.

The exact molecular mechanisms underlying superior cardiac rescue by the ΔH2-R15 minigene will have to wait until future in-depth studies. Nevertheless, we speculate that it may at least partially due to the presence of R16-19 in this minigene. Nigro et al studied 284 patients and found that deletion of exons 48 and 49 (R19) correlates with severe cardiac disease [23]. In a more recent study, Kaspar et al analyzed 78 patients and discovered the N-terminal domain and R17-19 might protect the heart. Deletion of one these two regions often result in early onset heart disease [33]. Numerous clinical studies on Becker muscular dystrophy (a mild form of DMD)

and X-linked dilated cardiomyopathy (a disease caused by selective dystrophin deficiency in the heart) from other groups also pointed towards a potential cardiac protective role of R16-19 [19-33]. Our results aligned well with these patient oriented studies. Collectively, these data suggest that R16-19 may represent a putative heart protection domain in dystrophin.

It is worth noting that the existence of the tissue-specific domain in dystrophin has been well documented in the literature. For example, repeats 16 and 17 are essential for anchoring nNOS to the sarcolemma in skeletal muscle [14]. The C-terminal domain appears to be required for normal electroretinography and mutations in the C-terminal domain often associate with cognitive deficiency [70, 71]. However, except for the nNOS-binding R16/17 domain for skeletal muscle, dystrophin tissue-specific domains have rarely been studied and/or validated in animal models. The study described here is the first to try to experimentally determine whether certain regions of dystrophin can result in better heart rescue. While our results are encouraging, additional studies are needed before we can draw a solid conclusion. Some of these studies may include exploration of cardiac-specific dystrophin interacting proteins such as cavin-1 and αB-crystalline [66]. Cavin-1 is particularly interesting because several recent studies suggest that cavin-1 deficiency contributes to the pathogenesis of cardiomyopathy and muscular dystrophy [72-74].

An intriguing finding of our study is the presence of myocardial hypertrophy in αMHC.ΔH2-R15 mice **(Table 1)**. While the molecular trigger for cardiac hypertrophy in αMHC.ΔH2-R15 mice remains elusive **(Figure 4)**, it certainly suggests a reverse of the disease course from heart failure associated dilated cardiomyopathy to compensatory hypertrophic remodeling [16, 17].

We would like to point out that we have used the transgenic approach in the hope of (1) comparing with our previously published data from αMHC.ΔH2-R19 transgenic mdx mice, and (2) more clearly delineating the cardiac specific effect of dystrophin R16-19. However, the transgenic approach cannot be directly applied to gene therapy. While the size of the ΔH2-R15 minigene (~ 7-kb) exceeds the packaging capacity of a single AAV vector, it can be expressed using various dual AAV vector strategies. Specifically, the minigene expression cassette can be split into two parts and separately packaged with two independent AAV virions. Co-delivery and intermolecular recombination would allow expression of the ΔH2-R15 minigene. Future studies with a set of ΔH2-R15 minigene dual AAV vectors will be necessary to further corroborate transgenic findings described here. Alternatively, the therapeutic benefit of R16-19 may be investigated using AAV-mediated expression of a micro-dystrophin gene. In this case, one will have to engineer a novel synthetic microgene (≤ 4-kb) that contains R16-19.

In summary, we have provided the first animal study evidence supporting inclusion of R16-19 in a therapeutic candidate gene could be beneficial for treating Duchenne cardiomyopathy.

Acknowledgements

This work was supported by Jackson Freel DMD Research Fund, Jesse's Journey-The Foundation for Gene and Cell Therapy and the Margaret Proctor Mulligan endowment to the University of Missouri. Supplementary funding was provided through grants from the National Institutes of Health (HL-91883, NS-90634). NW was partially supported by the life science fellowship, University of Missouri. FM is supported by a Marie-Curie senior fellowship from the EU H2020 program and by the National Institute for Health Research Biomedical Research Centre at Great Ormond Street Hospital for Children NHS Foundation Trust and University College London. We thank the University of Missouri Transgenic Animal Core for the help with generating the founder transgenic mice. NBW, JHS and DD designed the study. NBW, JHS, YL and YY performed research. FM contributed new reagents or analytic tools. NBW and DD analyzed data. DD and NBW wrote the paper. All authors edited paper and approved submission.

Author Disclosure Statement

D.D. is a member of the scientific advisory board for Solid Biosciences LLC and an equity holder of Solid Biosciences LLC. The Duan lab has received research supports from Solid Biosciences LLC.

References

1. Baxter P. Treatment of the heart in Duchenne muscular dystrophy. Dev Med Child Neurol 2006;48:163.
2. Cox GF, Kunkel LM. Dystrophies and heart disease. Curr Opin Cardiol 1997;12:329-343.
3. Pediatrics AAo. Cardiovascular health supervision for individuals affected by Duchenne or Becker muscular dystrophy. Pediatrics 2005;116:1569-1573.
4. Duan D. Challenges and opportunities in dystrophin-deficient cardiomyopathy gene therapy. Hum Mol Genet 2006;15 Spec No 2:R253-261.
5. Lai Y, Duan D. Progress in gene therapy of dystrophic heart disease. Gene Ther 2012;19:678-685.
6. Yue Y, Binalsheikh IM, Leach SB et al. Prospect of gene therapy for cardiomyopathy in hereditary muscular dystrophy. Expert opinion on orphan drugs 2016;4:169-183.
7. Gregorevic P, Blankinship MJ, Allen JM et al. Systemic delivery of genes to striated muscles using adeno-associated viral vectors. Nature medicine 2004;10:828-834.
8. Wang Z, Zhu T, Qiao C et al. Adeno-associated virus serotype 8 efficiently delivers genes to muscle and heart. Nature biotechnology 2005;23:321-328.
9. Yue Y, Ghosh A, Long C et al. A single intravenous injection of adeno-associated virus serotype-9 leads to whole body skeletal muscle transduction in dogs. Mol Ther 2008;16:1944-1952.
10. Yue Y, Pan X, Hakim CH et al. Safe and bodywide muscle transduction in young adult Duchenne muscular dystrophy dogs with adeno-associated virus. Hum Mol Genet 2015;24:5880-5890.

11. Duan D. Systemic delivery of adeno-associated viral vectors. Current opinion in virology 2016;21:16-25.
12. Harper SQ, Hauser MA, DelloRusso C et al. Modular flexibility of dystrophin: implications for gene therapy of Duchenne muscular dystrophy. Nat Med 2002;8:253-261.
13. England SB, Nicholson LV, Johnson MA et al. Very mild muscular dystrophy associated with the deletion of 46% of dystrophin. Nature 1990;343:180-182.
14. Lai Y, Thomas GD, Yue Y et al. Dystrophins carrying spectrin-like repeats 16 and 17 anchor nNOS to the sarcolemma and enhance exercise performance in a mouse model of muscular dystrophy. J Clin Invest 2009;119:624-635.
15. Bostick B, Yue Y, Long C et al. Cardiac expression of a mini-dystrophin that normalizes skeletal muscle force only partially restores heart function in aged mdx mice. Mol Ther 2009;17:253-261.
16. Nigro G, Comi LI, Politano L et al. The incidence and evolution of cardiomyopathy in Duchenne muscular dystrophy. Int J Cardiol 1990;26:271-277.
17. Papa AA, D'Ambrosio P, Petillo R et al. Heart transplantation in patients with dystrophinopathic cardiomyopathy: Review of the literature and personal series. Intractable Rare Dis Res 2017;6:95-101.
18. Bostick B, Yue Y, Duan D. Gender influences cardiac function in the mdx model of Duchenne cardiomyopathy. Muscle Nerve 2010;42:600-603.
19. Arbustini E, Diegoli M, Morbini P et al. Prevalence and characteristics of dystrophin defects in adult male patients with dilated cardiomyopathy. J Am Coll Cardiol 2000;35:1760-1768.
20. Palmucci L, Doriguzzi C, Mongini T et al. Dilating cardiomyopathy as the expression of Xp21 Becker type muscular dystrophy. J Neurol Sci 1992;111:218-221.

21. Melacini P, Fanin M, Danieli GA et al. Cardiac involvement in Becker muscular dystrophy. J Am Coll Cardiol 1993;22:1927-1934.
22. Yoshida K, Ikeda S, Nakamura A et al. Molecular analysis of the Duchenne muscular dystrophy gene in patients with Becker muscular dystrophy presenting with dilated cardiomyopathy. Muscle Nerve 1993;16:1161-1166.
23. Nigro G, Politano L, Nigro V et al. Mutation of dystrophin gene and cardiomyopathy. Neuromuscul Disord 1994;4:371-379.
24. Piccolo G, Azan G, Tonin P et al. Dilated cardiomyopathy requiring cardiac transplantation as initial manifestation of Xp21 Becker type muscular dystrophy. Neuromuscul Disord 1994;4:143-146.
25. Siciliano G, Fanin M, Angelini C et al. Prevalent cardiac involvement in dystrophin Becker type mutation. Neuromuscul Disord 1994;4:381-386.
26. Muntoni F, Di Lenarda A, Porcu M et al. Dystrophin gene abnormalities in two patients with idiopathic dilated cardiomyopathy. Heart 1997;78:608-612.
27. Melis MA, Cau M, Deidda F et al. Mutation of dystrophin gene in two families with X-linked dilated cardiomyopathy. Neuromuscul Disord 1998;8:244.
28. Todorova A, Constantinova D, Kremensky I. Dilated cardiomyopathy and new 16 bp deletion in exon 44 of the Dystrophin gene: the possible role of repeated motifs in mutation generation. American journal of medical genetics Part A 2003;120A:5-7.
29. Nakamura A, Yoshida K, Fukushima K et al. Follow-up of three patients with a large in-frame deletion of exons 45-55 in the Duchenne muscular dystrophy (DMD) gene. J Clin Neurosci 2008;15:757-763.

30. Miyazaki D, Yoshida K, Fukushima K et al. Characterization of deletion breakpoints in patients with dystrophinopathy carrying a deletion of exons 45-55 of the Duchenne muscular dystrophy (DMD) gene. J Hum Genet 2009;54:127-130.

31. Yazaki M, Yoshida K, Nakamura A et al. Clinical characteristics of aged Becker muscular dystrophy patients with onset after 30 years. European neurology 1999;42:145-149.

32. Tasaki N, Yoshida K, Haruta SI et al. X-linked dilated cardiomyopathy with a large hot-spot deletion in the dystrophin gene. Intern Med 2001;40:1215-1221.

33. Kaspar RW, Allen HD, Ray WC et al. Analysis of dystrophin deletion mutations predicts age of cardiomyopathy onset in becker muscular dystrophy. Circ Cardiovasc Genet 2009;2:544-551.

34. Bostick B, Yue Y, Long C et al. Prevention of dystrophin-deficient cardiomyopathy in twenty-one-month-old carrier mice by mosaic dystrophin expression or complementary dystrophin/utrophin expression. Circ Res 2008;102:121-130.

35. Wasala NB, Zhang K, Wasala LP et al. The FVB background does not dramatically alter the dystrophic phenotype of mdx mice. PLoS Curr 2015;7:pii: ecurrents.md.28266819ca28266810ec28266815fefcac28266767ea28266819a28263461c.

36. Yue Y, Skimming JW, Liu M et al. Full-length dystrophin expression in half of the heart cells ameliorates beta-isoproterenol-induced cardiomyopathy in mdx mice. Hum Mol Genet 2004;13:1669-1675.

37. Kodippili K, Vince L, Shin JH et al. Characterization of 65 epitope-specific dystrophin monoclonal antibodies in canine and murine models of duchenne muscular dystrophy by immunostaining and western blot. PLoS One 2014;9:e88280.

38. Wasala NB, Bostick B, Yue Y et al. Exclusive skeletal muscle correction does not modulate dystrophic heart disease in the aged mdx model of Duchenne cardiomyopathy. Hum Mol Genet 2013;22:2634-2641.

39. Li D, Yue Y, Lai Y et al. Nitrosative stress elicited by nNOSmu delocalization inhibits muscle force in dystrophin-null mice. J Pathol 2011;223:88-98.

40. Bostick B, Yue Y, Duan D. Phenotyping cardiac gene therapy in mice. Methods Mol Biol 2011;709:91-104.

41. Duan D, Rafael-Fortney JA, Blain A et al. Standard Operating Procedures (SOPs) for Evaluating the Heart in Preclinical Studies of Duchenne Muscular Dystrophy. J Cardiovasc Transl Res 2016;9:85-86.

42. Bostick B, Shin J-H, Yue Y et al. AAV-microdystrophin therapy improves cardiac performance in aged female mdx mice. Mol Ther 2011;19:1826-1832.

43. Mitchell GF, Jeron A, Koren G. Measurement of heart rate and Q-T interval in the conscious mouse. Am J Physiol 1998;274:H747-751.

44. Nigro G, Comi LI, Politano L et al. Cardiomyopathies associated with muscular dystrophies. In: Myology : basic and clinical. A Engel and C Franzini-Armstrong, eds. (McGraw-Hill, Medical Pub. Division, New York). 2004; pp. 1239-1256.

45. Yue Y, Wasala NB, Bostick B et al. 100-fold but not 50-fold dystrophin overexpression aggravates electrocardiographic defects in the mdx model of Duchenne muscular dystrophy. Mol Ther Methods Clin Dev 2016;3:16045.

46. Yin FC, Spurgeon HA, Rakusan K et al. Use of tibial length to quantify cardiac hypertrophy: application in the aging rat. Am J Physiol 1982;243:H941-947.

47. Rohini A, Agrawal N, Koyani CN et al. Molecular targets and regulators of cardiac hypertrophy. Pharmacological research 2010;61:269-280.

48. Balakumar P, Jagadeesh G. Multifarious molecular signaling cascades of cardiac hypertrophy: can the muddy waters be cleared? Pharmacological research 2010;62:365-383.

49. Barry SP, Davidson SM, Townsend PA. Molecular regulation of cardiac hypertrophy. The international journal of biochemistry & cell biology 2008;40:2023-2039.

50. Heineke J, Molkentin JD. Regulation of cardiac hypertrophy by intracellular signalling pathways. Nature reviews Molecular cell biology 2006;7:589-600.

51. Kehat I, Molkentin JD. Molecular pathways underlying cardiac remodeling during pathophysiological stimulation. Circulation 2010;122:2727-2735.

52. Yokota T, Wang Y. p38 MAP kinases in the heart. Gene 2016;575:369-376.

53. Marber MS, Rose B, Wang Y. The p38 mitogen-activated protein kinase pathway--a potential target for intervention in infarction, hypertrophy, and heart failure. J Mol Cell Cardiol 2011;51:485-490.

54. Liang Q, Molkentin JD. Redefining the roles of p38 and JNK signaling in cardiac hypertrophy: dichotomy between cultured myocytes and animal models. J Mol Cell Cardiol 2003;35:1385-1394.

55. Shimizu I, Minamino T. Physiological and pathological cardiac hypertrophy. J Mol Cell Cardiol 2016;97:245-262.

56. Pillai VB, Sundaresan NR, Gupta MP. Regulation of Akt signaling by sirtuins: its implication in cardiac hypertrophy and aging. Circ Res 2014;114:368-378.

57. Salazar NC, Chen J, Rockman HA. Cardiac GPCRs: GPCR signaling in healthy and failing hearts. Biochim Biophys Acta 2007;1768:1006-1018.

58. Kang M, Chung KY, Walker JW. G-protein coupled receptor signaling in myocardium: not for the faint of heart. Physiology (Bethesda) 2007;22:174-184.

59. Esposito G, Rapacciuolo A, Naga Prasad SV et al. Cardiac hypertrophy: role of G protein-coupled receptors. Journal of cardiac failure 2002;8:S409-414.

60. Maillet M, van Berlo JH, Molkentin JD. Molecular basis of physiological heart growth: fundamental concepts and new players. Nat Rev Mol Cell Biol 2013;14:38-48.

61. Crisp A, Yin H, Goyenvalle A et al. Diaphragm rescue alone prevents heart dysfunction in dystrophic mice. Hum Mol Genet 2011;20:413-421.

62. Townsend D, Yasuda S, Chamberlain J et al. Cardiac consequences to skeletal muscle-centric therapeutics for Duchenne muscular dystrophy. Trends Cardiovasc Med 2009;19:50-55.

63. Lai Y, Zhao J, Yue Y et al. alpha2 and alpha3 helices of dystrophin R16 and R17 frame a microdomain in the alpha1 helix of dystrophin R17 for neuronal NOS binding. Proc Natl Acad Sci U S A 2013;110:525-530.

64. Xu KY, Huso DL, Dawson TM et al. Nitric oxide synthase in cardiac sarcoplasmic reticulum. Proc Natl Acad Sci U S A 1999;96:657-662.

65. Kanai AJ, Pearce LL, Clemens PR et al. Identification of a neuronal nitric oxide synthase in isolated cardiac mitochondria using electrochemical detection. Proc Natl Acad Sci U S A 2001;98:14126-14131.

66. Johnson EK, Zhang L, Adams ME et al. Proteomic analysis reveals new cardiac-specific dystrophin-associated proteins. PLoS One 2012;7:e43515.

67. Lai Y, Zhao J, Yue Y et al. Partial restoration of cardiac function with ΔPDZ nNOS in aged mdx model of Duchenne cardiomyopathy. Hum Mol Genet 2014;23:3189-3199.

68. Meng H, Leddy JJ, Frank J et al. The association of cardiac dystrophin with myofibrils/Z-disc regions in cardiac muscle suggests a novel role in the contractile apparatus. J Biol Chem 1996;271:12364-12371.

69. Zhang Y, Yue Y, Li L et al. Dual AAV therapy ameliorates exercise-induced muscle injury and functional ischemia in murine models of Duchenne muscular dystrophy. Hum Mol Genet 2013;22:3720-3729.

70. Pillers DA. Dystrophin and the retina. Mol Genet Metab 1999;68:304-309.

71. Ricotti V, Mandy WP, Scoto M et al. Neurodevelopmental, emotional, and behavioural problems in Duchenne muscular dystrophy in relation to underlying dystrophin gene mutations. Dev Med Child Neurol 2016;58:77-84.

72. Rajab A, Straub V, McCann LJ et al. Fatal cardiac arrhythmia and long-QT syndrome in a new form of congenital generalized lipodystrophy with muscle rippling (CGL4) due to PTRF-CAVIN mutations. PLoS genetics 2010;6:e1000874.

73. Taniguchi T, Maruyama N, Ogata T et al. PTRF/Cavin-1 Deficiency Causes Cardiac Dysfunction Accompanied by Cardiomyocyte Hypertrophy and Cardiac Fibrosis. PLoS One 2016;11:e0162513.

74. Ding SY, Liu LB, Pilch PF. Muscular dystrophy in PTFR/cavin-1 null mice. Jci Insight 2017;2.

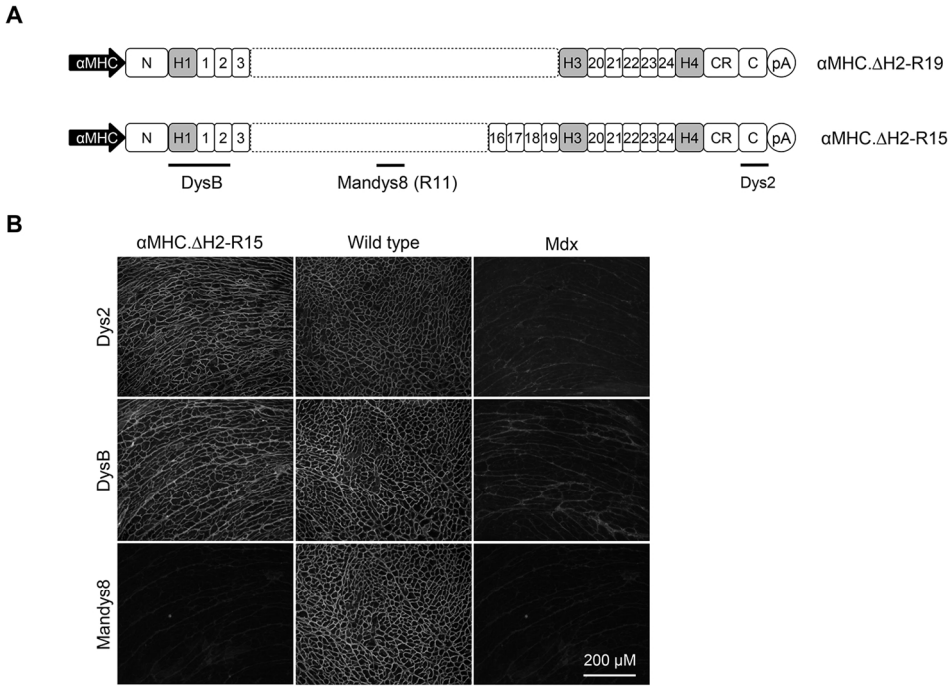

Figure 1 A-B

140x96mm (300 x 300 DPI)

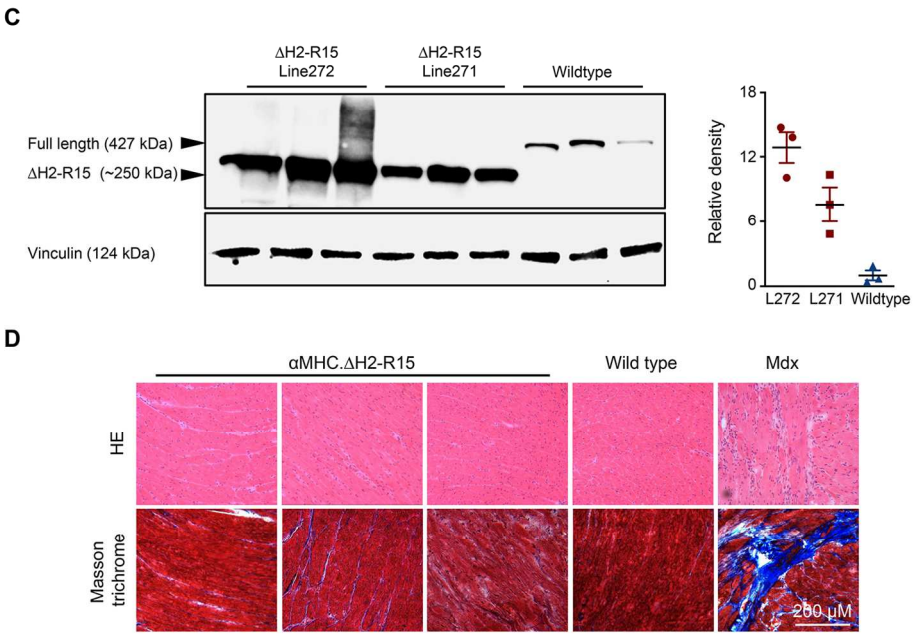

Figure 1 C-D

140x89mm (300 x 300 DPI)

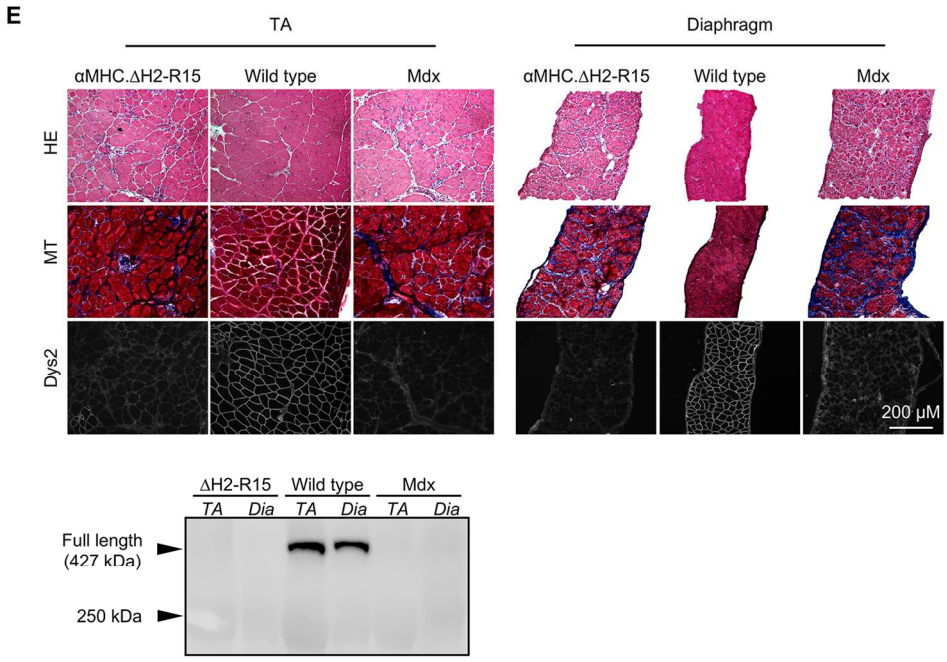

Figure 1 E

140x93mm (300 x 300 DPI)

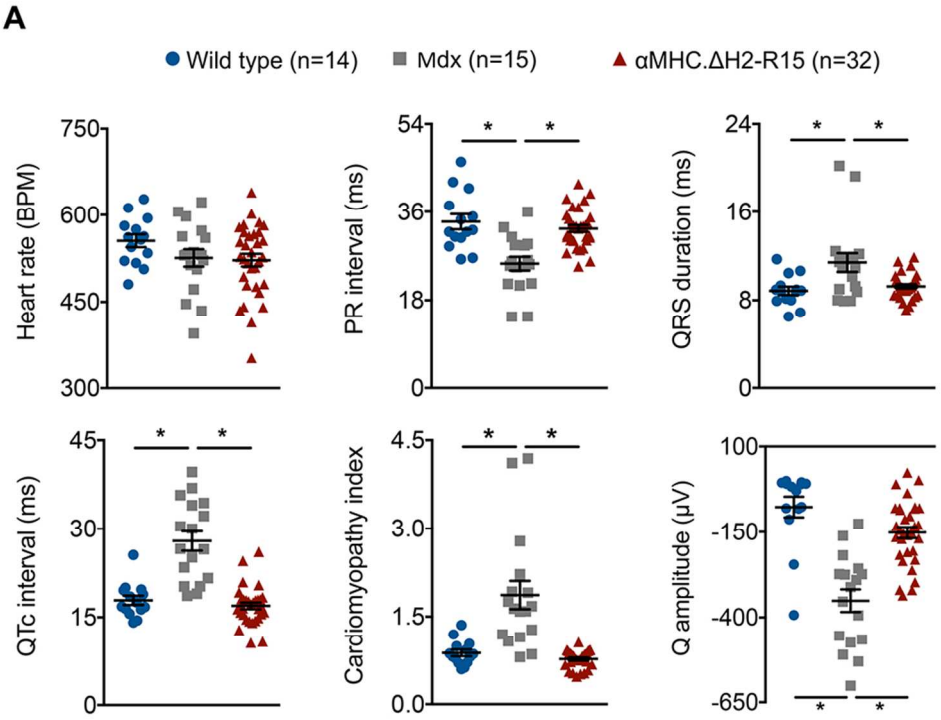

Figure 2A

90x66mm (300 x 300 DPI)

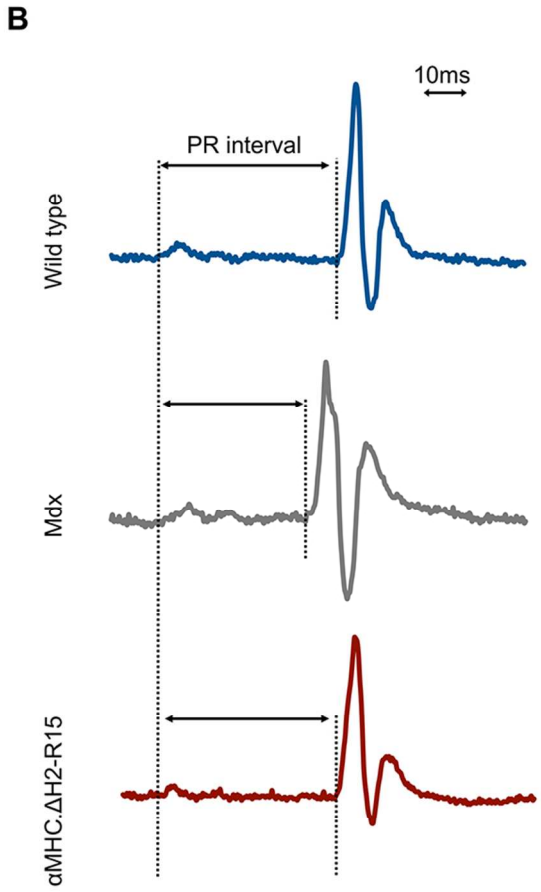

Figure 2B

90x82mm (300 x 300 DPI)

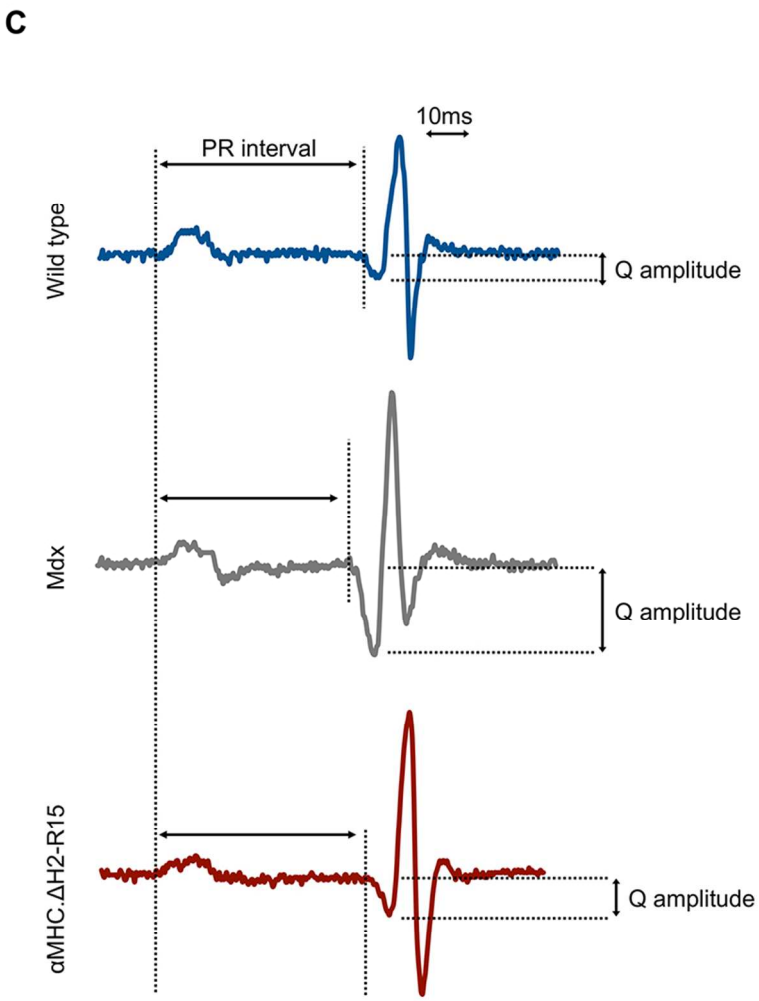

Figure 2C

90x93mm (300 x 300 DPI)

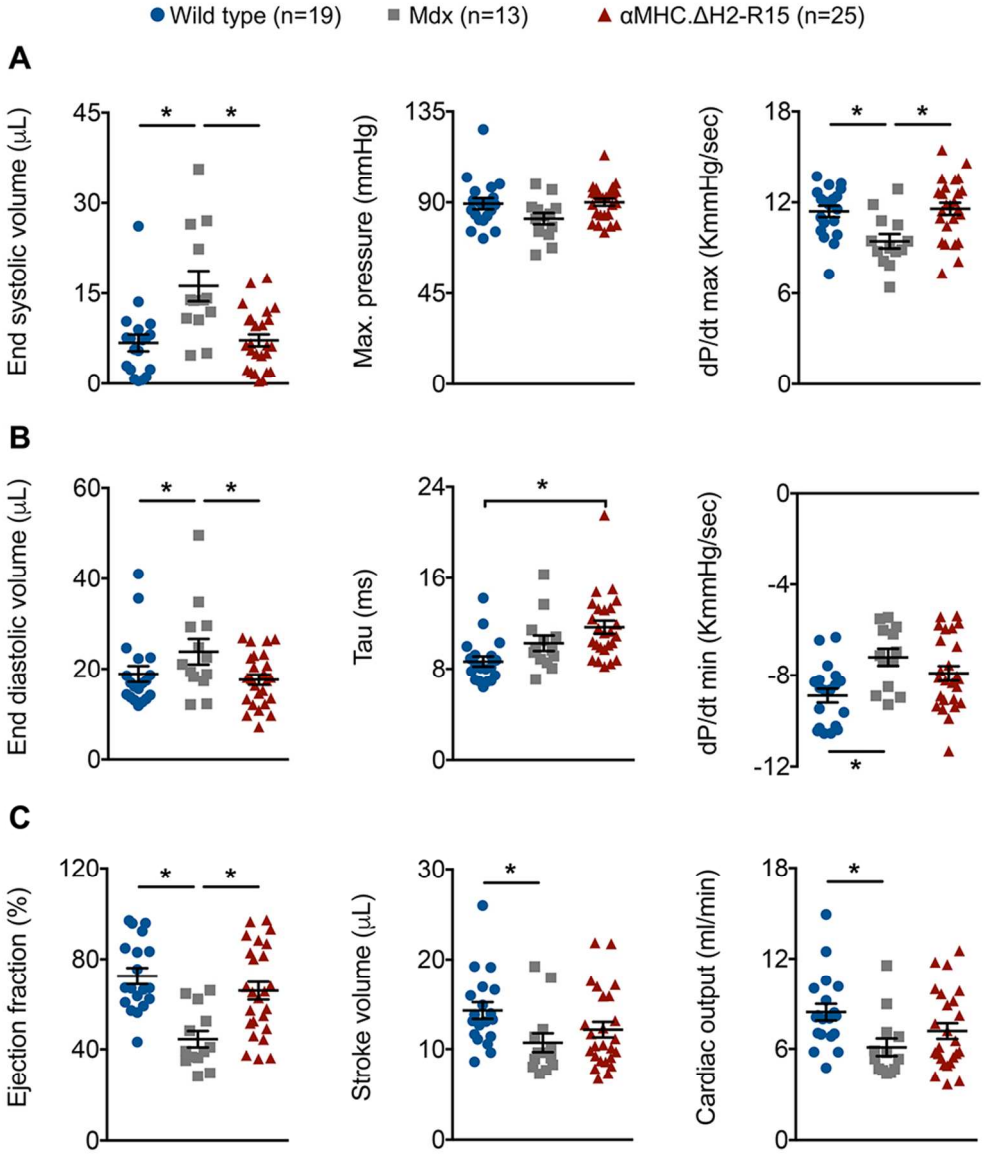

Figure 3A-C

90x107mm (300 x 300 DPI)

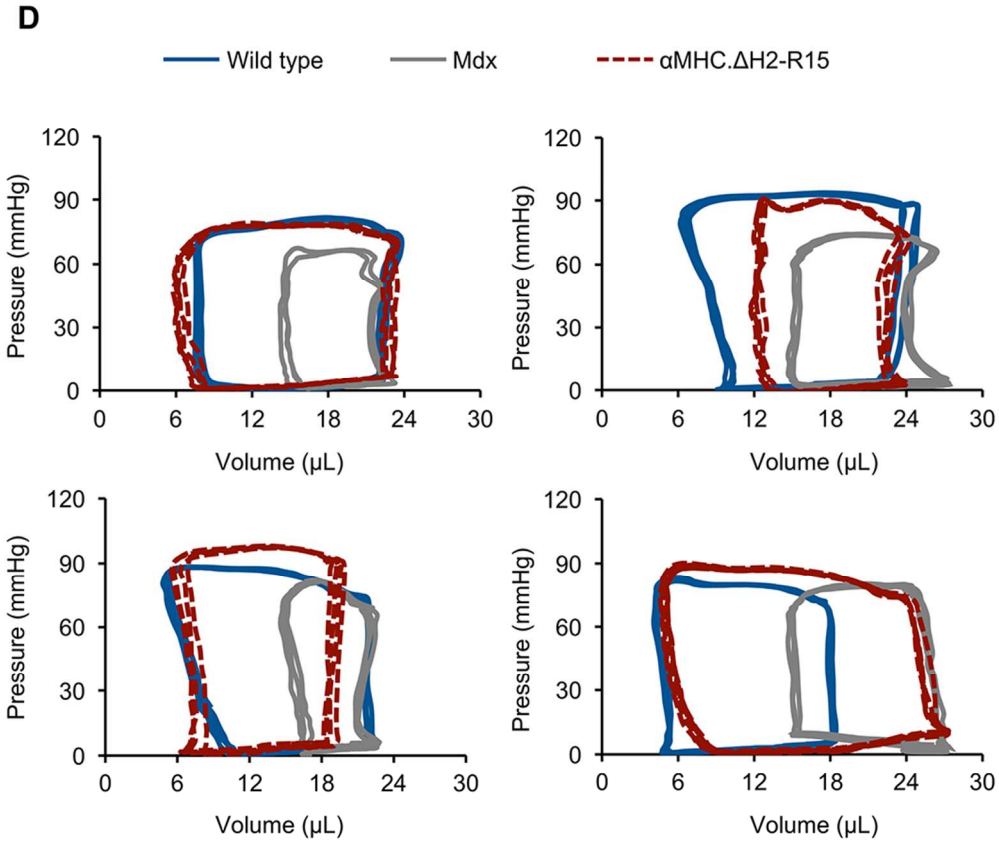

Figure 3D

90x79mm (300 x 300 DPI)

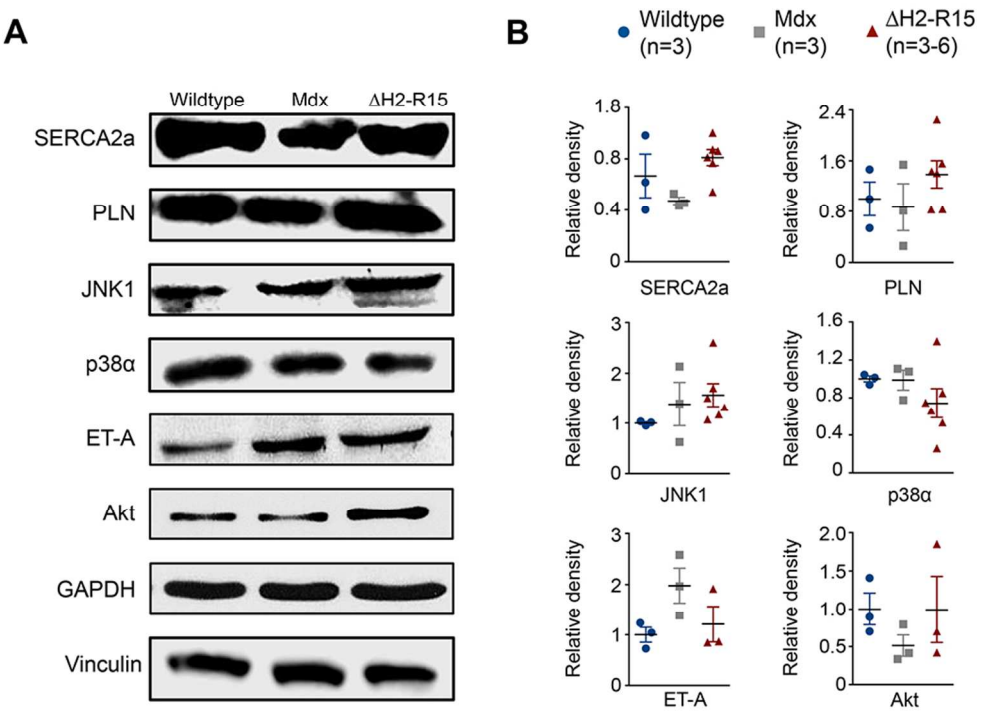

Figure 4

90x63mm (300 x 300 DPI)

Figure Legends

Figure 1. Heart-specific expression of ΔH2-R15 mini-dystrophin ameliorated cardiac but not skeletal muscle pathology. A, Illustrations of ΔH2-R19 and ΔH2-R15 mini-dystrophin. Dotted box marks the region deleted from full-length dystrophin. Mini-dystrophin expression is under the control of the heart-specific α-myosin heavy chain (αMHC) promoter. **B,** Representative photomicrographs of dystrophin immunofluorescence staining in the heart of wild type, mdx and αMHC.ΔH2-R15 transgenic mdx mice. DysB, Dys2 and Mandys8 are dystrophin monoclonal antibodies used in the study. DysB and Dys2 recognize H1-R2 and the C-terminal domain of dystrophin, respectively. The epitope for Mandys8 (R11) is absent in ΔH2-R15 mini-dystrophin. **C,** Representative western blots of dystrophin (Dys2) in the heart of two lines of αMHC.ΔH2-R15 transgenic mdx mice and normal wild type control mice. The right panel shows dystrophin densitometry quantification. **D,** Representative photomicrographs of HE and Masson trichrome staining in the heart of wild type, mdx and αMHC.ΔH2-R15 transgenic mdx mice. **E,** Representative photomicrographs of HE, Masson trichrome (MT) and Dys2 immunofluorescence staining in the tibialis anterior muscle (TA) and diaphragm of wild type, mdx and αMHC.ΔH2-R15 transgenic mdx mice (top three panels). The bottom panel shows representative dystrophin (Dys2) western blots from skeletal muscle (TA and diaphragm) of wild type, mdx and αMHC.ΔH2-R15 transgenic mdx mice.

Figure 2. ΔH2-R15 mini-dystrophin completely rescued ECG abnormalities. A, Quantitative evaluation of the heart rate, PR interval, QRS duration, QTc interval, Q amplitude and cardiomyopathy index. Asterisk, significantly different from the indicated group. **B,**

Representative lead II ECG tracing from wild type, mdx and αMHC.ΔH2-R15 transgenic mdx mice. The PR interval was reduced in the mdx mouse but normalized in αMHC.ΔH2-R15 transgenic mdx mouse. **C,** Representative lead I ECG tracing from wild type, mdx and αMHC.ΔH2-R15 transgenic mdx mice. The deep Q wave in the mdx mouse was normalized in αMHC.ΔH2-R15 transgenic mdx mice.

Figure 3. ΔH2-R15 mini-dystrophin improved the left ventricular hemodynamics. A, Quantitative evaluation of systolic function. **B,** Quantitative evaluation of diastolic function. **C,** Quantitative evaluation of overall heart function in wild type, mdx and αMHC.ΔH2-R15 transgenic mdx mice. Asterisk, significantly different from the indicated group. **D,** Selected pressure-volume loops from wild type, mdx and αMHC.ΔH2-R15 transgenic mdx mice. Different scenarios (including some extreme cases) are presented to reflect individual differences. For example, in the top right panel the PV loop from the transgenic mouse is almost identical to that of a normal mouse but the PV loop from the mdx mouse does not show the typical enlargement of the end-diastolic volume. The top left panel is the representative PV loops from all experimental groups.

Figure 4. Evaluation of calcium handling proteins and cardiac hypertrophy-related signaling proteins. A, Representative immunoblots for sarcoplasmic/endoplasmic reticulum calcium ATPase 2a (SERCA2a), phospholamban (PLN), c-jun N-terminal kinase 1 (JNK1), endothelin receptor A (ET-A). Glyceraldehyde 3-phosphate dehydrogenase (GAPDH) or

vinculin was used the loading control. **B,** Densitometry quantification of the expression level (N=3-6 for each group).

Tables

Table 1. Weights and weight ratios

	FVB	Mdx/FVB	αMHC.ΔH2-R15
Sample Size (N)	25	13	38
Age (m)	23.50 ± 0.17	21.03 ± 0.32[a]	23.22 ± 0.16
BW (g)	29.05 ± 1.11	27.08 ± 1.03	30.13 ± 1.10
HW (mg)	113.16 ± 3.23	122.28 ± 3.97	128.38 ± 3.09[b]
VW (mg)	103.20± 3.05	112.59 ± 3.60	118.95 ± 2.83[b]
TL (mm)	18.79 ± 0.08	19.05 ± 0.07	18.90 ± 0.05
TW (mg)	36.79 ± 0.90[a]	32.35 ± 0.96	31.83 ± 0.86
HW/BW (mg/g)	4.00 ± 0.15	4.57 ± 0.18	4.34 ± 0.13
HW/TL (mg/mm)	6.02 ± 0.17	6.38 ± 0.21	6.58 ± 0.16[b]
HW/TW (mg/g)	3.09 ± 0.08[a]	3.81 ± 0.13	4.12 ± 0.12
VW/BW (mg/g)	3.66 ± 0.14	4.20 ± 0.16	4.02 ± 0.12
VW/TL (mg/mm)	5.48 ± 0.16	5.89 ± 0.19	6.10 ± 0.15[b]
VW/TW (mg/g)	2.81 ± 0.07[a]	3.51 ± 0.12	3.82 ± 0.11

Abbreviations: BW, body weight; HW, heart weight; VW, ventricle weight; TL, tibia length; TW, anterior tibialis muscle weight.

[a], significantly different from other two groups

[b], significantly different from FVB

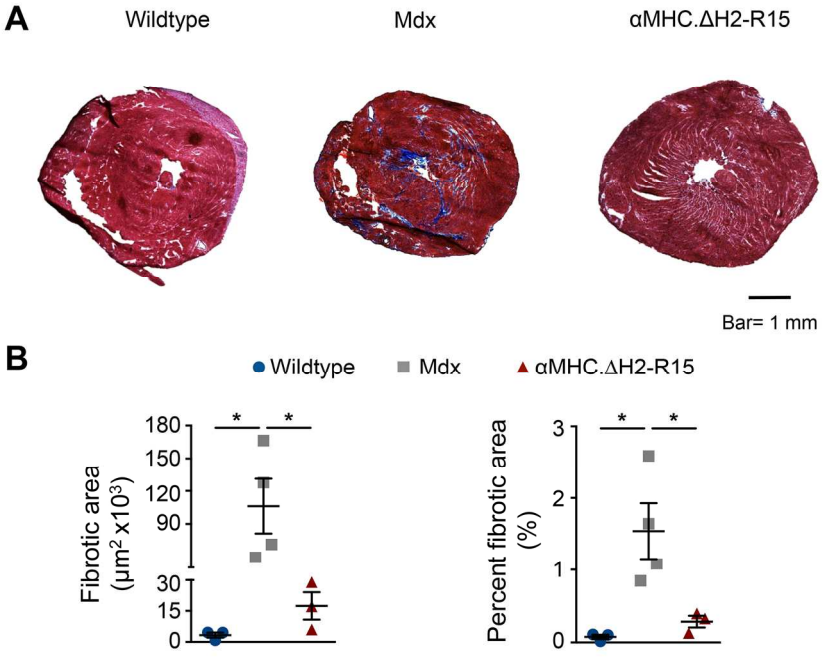

Supplementary figure 1

180x119mm (300 x 300 DPI)

Supplementary Figure legend

Supplementary Figure 1. Myocardial fibrosis is significantly reduced in αMHC.ΔH2-R15 transgenic mice. A, Representative photomicrographs of whole heart cross section of Masson trichrome staining. **B,** Quantification of area of fibrosis in each strain. The left panel shows the absolute area of fibrotic area in the heart and the right panel shows the percentage of fibrotic area in the whole heart cross section.

Supplementary Table

Supplementary Table 1. Hemodynamic comparison of two transgenic lines with wild type and mdx included as references.

	Wild type	Mdx	αMHC.ΔH2-R15 L271	αMHC.ΔH2-R15 L272
Sample Size (N)	19	13	19	6
ESV (µL)	6.79± 1.35	16.19 ± 2.43	7.30± 1.15	6.91 ± 1.76
MaxP (mmHg)	89.36 ± 2.7	81.93 ± 2.69	89.92 ± 2.05	90.46 ± 2.90
dP/dt max (KmmHg/sec)	11.40 ± 0.36	9.40± 0.46	11.80 ± 0.43	10.88± 0.83
EDV (µL)	18.89 ± 1.73	23.83± 2.72	17.84 ± 1.36	16.87 ± 2.02
dP/dt min (mmHg/sec)	-8.90 ± 0.30	-7.20 ± 0.68	-8.21 ± 0.32	-6.95 ± 0.68
Tau (ms)	8.66 ± 0.43	10.26 ± 0.65	12.24 ± 0.47	13.02 ± 1.72
SV (µL)	14.30 ± 0.91	10.71 ± 1.01	12.24 ± 0.93	11.93 ± 1.94
EF (%)	72.54 ± 0.91	44.51 ± 3.49	66.42 ± 4.41	64.62 ± 8.04
CO (mL/sec)	8.45 ± 0.54	6.11± 0.56	7.36 ± 0.55	6.66± 1.18

ESV, end systolic volume; MaxP, maximum pressure; dP/dt max, maximum dP/dt; EDV, end-diastolic volume; dP/dt min, minimum dP/dt; Tau, isovolumetric relaxation time constant; SV, stroke volume; EF, ejection fraction; CO, cardiac output. The statistical analysis between the two transgenic lines (line L271 and line L272) failed to yield any significant difference between the two lines.